ehp ENVIRONMENTAL HEALTH PERSPECTIVES
http://www.ehponline.org

Disruption of Aryl Hydrocarbon Receptor Homeostatic Levels during Embryonic Stem Cell Differentiation Alters Expression of Homeobox Transcription Factors that Control Cardiomyogenesis

Qin Wang, Jing Chen, Chia-I Ko, Yunxia Fan, Vinicius Carreira, Yinglei Chen, Ying Xia, Mario Medvedovic, and Alvaro Puga

http://dx.doi.org/10.1289/ehp.1307297

Received: 30 June 2013
Accepted: 19 September 2013
Advance Publication: 20 September 2013

NIH National Institute of Environmental Health Sciences

Disruption of Aryl Hydrocarbon Receptor Homeostatic Levels during Embryonic Stem Cell Differentiation Alters Expression of Homeobox Transcription Factors that Control Cardiomyogenesis

Qin Wang, Jing Chen, Chia-I Ko, Yunxia Fan, Vinicius Carreira, Yinglei Chen, Ying Xia, Mario Medvedovic, and Alvaro Puga

Department of Environmental Health and Center for Environmental Genetics, University of Cincinnati College of Medicine, Cincinnati, Ohio, USA

Address correspondence to:

Alvaro Puga

Department of Environmental Health and Center for Environmental Genetics

University of Cincinnati College of Medicine

3223 Eden Avenue, Cincinnati, Ohio, 45267

Phone: 513.558.0916

Fax: 513.558.0925

E-mail: Alvaro.Puga@uc.edu

Running Title: The AHR Regulates Cardiomyogenesis

Acknowledgments: We thank Miral Patel and Saikumar Karyala for their excellent help with RNA.seq. We thank Drs. Andras Nagy and Marina Gertsenstein, Mount Sinai Hospital and Samuel Lunenfeld Research Institute, Toronto, Canada for the C57BL/6N-C2 ES cells, and Drs. Agapios Sachinidis and Michael Jesudoss, Institute of Neurophysiology, University of Cologne, Germany, for the PuroIRESeGFP vector for promoter sorting cell selection. We also thank Drs.

Hisaka Kurita, Francisco-Javier Sánchez-Martín and Jerry Ovesen for a critical reading of the manuscript. Genome-wide RNA.seq data has been submitted to the GEO database with access URL http://www.ncbi.nlm.nih.gov/geo/query/acc.cgi?acc=GSE47964

This research was supported by NIEHS grants R01 ES06273, R01 ES10807, the NIEHS Center for Environmental Genetics grant P30 ES06096. V.C. was supported by NIEHS T32 ES016646 Gene-Environment Interactions Training Grant. The authors declare that they have no competing financial interests.

Abstract

Background. The aryl hydrocarbon receptor (AHR) is a ligand activated transcription factor that regulates the expression of xenobiotic detoxification genes and is a critical mediator of gene-environment interactions. Many AHR target genes identified by genome-wide gene expression profiling have morphogenetic functions, suggesting that AHR may play a role in embryonic development.

Objectives. To characterize the developmental functions of the AHR we studied the consequences of AHR activation by the agonist 2,3,7,8-tetrachlorodibenzo-*p*-doxin (TCDD), and of its repression by the antagonists 6,2,4-trimethoxyflavone (TMF) and CH223191 or by shRNA-mediated AHR knockdown during spontaneous embryonic stem (ES) cell differentiation into cardiomyocytes.

Methods. We generated an AHR-positive cardiomyocyte lineage differentiated from mouse ES cells that expresses puromycin resistance and enhanced green fluorescent protein (eGFP) under the control of the *Cyp1a1* promoter. We used RNA.Seq to analyze temporal trajectories of TCDD-dependent global gene expression in these cells during differentiation.

Results. Activation, inhibition and knockdown of AHR significantly inhibited the formation of contractile cardiomyocyte nodes. Global expression analysis of AHR positive cells showed that activation of the AHR/TCDD axis disrupts the concerted expression of genes that regulate multiple signaling pathways involved in cardiac and neural morphogenesis and differentiation, including dozens of genes encoding homeobox transcription factors and Polycomb and Trithorax Group proteins.

Conclusions. Disruption of AHR expression levels results in gene expression changes that perturb cardiomyocyte differentiation. The main function of the AHR during development

appears to be the coordination of a complex regulatory network responsible for attainment and maintenance of cardiovascular homeostasis.

Introduction

The theory of the developmental origins of adult disease proposes that the environment encountered during fetal life and infancy permanently changes the body's structure, function and metabolism and shapes the long-term control of tissue physiology and homeostasis (Barker 2007). Accordingly, damage during fetal life or infancy resulting from maternal stress, poor nutrition or exposure to environmental pollutants, such as dioxin, may be at the heart of adult onset disease. Work in many laboratories has shown that the young are more sensitive to dioxin than the adult and that exposure to TCDD, the prototypical dioxin, during development results in disease conditions in adult fish (Plavicki et al. 2013), birds (Walker and Catron 2000) and mammals (Kopf and Walker 2009), including humans, in which dioxin exposure reduces fertility and negatively affect pregnancy outcomes across multiple generations (Bruner-Tran and Osteen 2011). The developmental toxicity of TCDD is of greater concern for humans because pregnant women transfer a fraction of their dioxin body burden to the fetus during pregnancy and to the postnatal infant via breastfeeding (Schecter et al. 2001). In addition, dioxin-like organochlorinated compounds are epidemiologically associated with low birth weight and respiratory distress (Lai et al. 2002) as well as cardiac malformations (Dummer et al. 2003). Infants born to mothers living near incinerators that emit complex mixtures of dioxins, furans, particulates and heavy metals exhibited a higher incidence of lethal congenital heart diseases. Other studies have shown an epidemiological association between the incidence of hypoplastic left heart syndrome and maternal exposure to halogenated hydrocarbons**,** dioxins and polychlorinated biphenyls during pregnancy (Kuehl and Loffredo 2006).

Most biological effects of TCDD are mediated by the AHR, a ligand activated transcription factor and a member of the basic-region-helix-loop-helix PER/ARNT/SIM (bHLH-PAS)

superfamily of transcription factors. Members of this superfamily function as sensors of extracellular signals and environmental stresses affecting growth and development (Gu et al. 2000). Activation by TCDD causes receptor translocation to the nucleus, dissociation from its cytosolic chaperones and heterodimerization with its AHR Nuclear Translocator (ARNT) partner, also a member of the bHLH/PAS superfamily (Reyes et al. 1992). Binding of AHR-ARNT complexes to AHR binding sites in the promoters of target genes recruits transcription cofactors and associated chromatin remodeling proteins and signals initiation of gene transcription (Schnekenburger et al. 2007). Increasing evidence indicates that in addition to the well-known xenobiotic metabolism genes in the Cyp1 family of cytochromes P450, there are other AHR transcriptional targets, including genes involved in cell cycle regulation and morphogenetic processes, that may play a vital function during embryonic development (Sartor et al. 2009b). In this context, following a complex alternating pattern of activation and repression in the preimplantation mouse embryo (Wu et al. 2002), AHR expression can be demonstrated in the post-implantation embryo as early as gestation day (GD) 9.5, followed by widespread expansion into almost all developing organs including brain, heart, liver, somites and branchial arches (Abbott et al. 1995).

The AHR is a major contributor to cardiovascular homeostasis in all species studied to date. In mice, fish and avian embryos, the heart is a TCDD target during fetal development, which causes reduced cardiomyocyte proliferation, altered fetal heart size and disrupts neovascularization (Ivnitski-Steele and Walker 2005). *In utero* exposure to TCDD increases the susceptibility to cardiovascular dysfunction in adult life (Aragon et al. 2008). Consistent with the concept that the AHR is a major player in cardiac function, knockout of the *Ahr* gene in mice disrupts cardiovascular homeostasis, causing pathological cardiac hypertrophy (Lund et al. 2003).

To address the hypothesis that AHR activation by TCDD during embryonic development disrupts expression of genes critical to cardiac differentiation, we generated an AHR-positive embryonic stem cell lineage that expresses puromycin resistance and eGFP under the control of the AHR-responsive *Cyp1a1* promoter. Activation of the AHR/TCDD axis in these cells disrupts the concerted expression of genes that regulate multiple signaling pathways involved in cardiac and neural morphogenesis and differentiation, including dozens of genes encoding homeobox transcription factors and Polycomb and Trithorax Group genes. Functional analysis of those genes suggests that homeostatic levels of AHR establish a complex regulatory network that controls various aspects of embryonic development, including cardiomyocyte differentiation.

Materials and Methods

Animals and TCDD exposure.

C57BL/6J mice were housed in the Experimental Laboratory Animals Medical Services at the University of Cincinnati under controlled conditions of temperature, humidity, and lighting, and provided standard mouse chow and water ad libitum. All experimental procedures conducted with these animals have been approved by the University of Cincinnati Animal Care and Use Committee. Animals were treated humanely and with regard for alleviation of suffering. Female mice were mated overnight and on GD5.5 pregnant dams were treated with either corn oil vehicle or with 5 or 50 µg TCDD/kg in corn oil by oral gavage. Based on previous determinations using isotopically labeled TCDD, these doses to the pregnant dam correspond to doses of 1.7 ng/kg and 17 ng/kg, respectively, to the embryos (Weber and Birnbaum 1985). For

analysis of AHR expression, the uteri of pregnant dams were harvested on GD7.5 and prepared for immunofluorescence detection as described below.

Culture of embryonic stem cells, in vitro differentiation and treatments.

Undifferentiated C57BL/6N-C2 ES cells (Gertsenstein et al. 2010) were maintained in ES medium, consisting of high glucose Dulbecco's minimal essential medium (DMEM) (Gibco) supplemented with 15% ES cell qualified Serum (Knockout Serum Replacement; Gibco, Carlsbad, CA), 2 mM glutamine, 1% nonessential amino acids, 100 U/ml penicillin, 100 μg/ml streptomycin, 0.1 mM β-mercaptoethanol, and 1000 U/ml ESGRO (LIF, Bioscience Research Reagents, Temecula, CA)). Cells were seeded in 0.1% gelatin-coated plates at 37°C, 95% humidity with 5% CO_2, and passaged every second or third day. Cell differentiation was initiated on day 0 by first forming embryoid bodies in hanging drops. Cells were transferred to DMEM medium without LIF supplemented with 15% non-ES qualified fetal bovine serum and suspended at a concentration of 40,000 - 70,000 cells/ml. Sixty 20-μl aliquots were pipetted onto the inner surface of a bacterial Petri dish lid and the lid was inverted over the bottom plate containing 15 ml PBS to provide humidity. Plates were incubated at 37°C for 3 days and thereafter the embryoid bodies (EBs) were flushed with differentiation medium and incubated in 24-well or 10-cm plates for varying periods of time. When needed, cultures were treated with TCDD in the 10 pM to 1 nM concentration range, commonly used for tissue culture work with the high-affinity Ah receptor of C57BL/6 mice. Treatments were for the length of time and at the final concentrations specified for each experiment or with the same volume of DMSO vehicle, used as a control, never to exceed 0.05 % of the final volume. To measure cardiomyocyte contractility, EBs were individually plated on wells of 24-well plates, allowed to differentiate in the presence of the indicated concentrations of TCDD or vehicle, and visually scored daily for

the presence of beating cell clusters. Beating became evident starting on day 6-7 and became maximal by day 10-11. If a well had more than one beating cluster it was scored as a single beating EB. Beating and non-beating areas of differentiated EBs were manually dissected under a dissecting microscope. In some experiments, differentiating cells were treated with the AHR antagonists TMF (Indofine Chemical Co., Hillsborough, NJ), or CH223191 (Chembridge, San Diego, CA) at the concentrations indicated in the figure legends.

shRNA knockdown of Ahr expression.

The validated lentiviral shRNA construct targeting *Ahr* transcripts TRCN0000055410 from the Mission ShRNA Lentiviral Collection (Sigma-Aldrich, St. Louis, MO) and a non-silencing control construct were purchased from the Lentivirus-shRNA Core of the Cincinnati Children's Hospital Medical Center. Mouse pluripotent ES cells were infected with these viruses in the presence of 8 µg/ml polybrene and stable AHR-knockdown ES cells were selected for resistance to 3 µg/ml of puromycin. The efficiency of knockdown was determined by immunobloting.

Preparation of whole cell extracts for immunoblotting.

Cells were washed and harvested in PBS containing 1X Complete Protease inhibitor and lysed in 300 µl NETN (100 mM NaCl, 20 mM Tris pH 8.0, 1 mM EDTA, 0.5% NP-40, and 1X Complete Protease inhibitor). After lysis, cells were sonicated on ice three times for 10 seconds each with a Fisher Scientific Sonic Dismembrator 60. Protein concentrations were measured using the Pierce BCA protein assay (Thermo Scientific, Flrence, KY). Protein extract aliquots of 50 µg were analyzed by SDS-polyacrylamide gel electrophoresis, transferred to polyvinylidene fluoride membranes and probed for AHR (Enzo Life Sciences, Inc. Farmingdale, NY) and β-actin (Sigma Aldrich).

Immunofluorescence.

For immunofluorescence studies, cells were seeded on 10-mm glass coverslips, fixed with 4% paraformaldehyde in PBS for 20 min, permeabilized with 0.1% triton X-100 for 20 min, blocked with 5% BSA for 0.5 hours, and incubated with first antibody at 4°C overnight. After washing, coverslips were stained with Alexa 488- or Alexa 567-labeled secondary antibodies and Hoechst solution. The cells were examined and images were captured using a Zeiss Axio microscope. At least five fields were evaluated for each treatment group. For the analysis of AHR localization by immunofluorescence, three-day old EBs were collected by low-speed centrifugation, rinsed once with PBS and the pellet fixed in 4% paraformaldehyde (Sigma-Aldrich), embedded in HistoGel (Thermo Scientific) and 5-µm sections were used for analysis. Antibodies used were directed against GATA4 (Santa Cruz Biotechnology, Santa Cruz, CA), cardiomyocytes (MF20) (Developmental Studies Hybridoma Bank at the University of Iowa), keratin-18 (Thermo Scientific), AHR (Enzo Life Sciences, Inc.), cardiac troponin T (Thermo Scientific), SHOX2 (Santa Cruz Biotechnology), and NKX2-5 (Santa Cruz Biotechnology). Mouse gravid uteri (GD7.5) were rinsed in PBS, adhered to white filter paper for proper orientation, and fixed in 4% paraformaldehyde overnight. Following fixation, uterine horns were dissected transversally to include implantation sites. Samples were then routinely processed for histopathology, that is, dehydrated, clarified, embedded in paraffin (embryos oriented longitudinally to the plane of section), and 5-µm sections prepared. Deparaffinized and rehydrated sections were boiled in 10 mM citrate, pH 6, for 10 min and allowed to cool to room temperature. Sections were blocked in 5% BSA in PBS pH 7.4 for 30 minutes at room temperature. Blocked sections were incubated overnight with primary antibody at 4°C, washed 3 times with PBS, incubated for 1 hour at room temperature with the appropriate fluorescently-labeled secondary antibody (Invitrogen) diluted in

5% BSA in PBS, washed again, and a coverslip was affixed with DAPI-containing mounting medium. Micrographs were taken using a Zeiss Axio Scope.A1 microscope equipped with an AxioCam ICm1 and Zeiss Zen software.

Total RNA isolation, reverse transcription and real-time RT-PCR.

Total RNA was extracted with the RNeasy Mini Kit (Qiagen, Valencia, CA) according to the manufacturer's specifications. First-strand complementary DNAs (cDNAs) were synthesized from 10 µg of total RNA in a volume of 15 µl containing 1X reverse transcriptase buffer, 7 mM random hexamers primer, 0.5 mM dNTP mix, 10 mM dithiothreitol, 5 mM $MgCl_2$, 20 U of RNase inhibitor (RNasin, Promega, Madison, WI), and 100 U of SuperScript III reverse transcriptase (Invitrogen, Carlsbad, CA). Samples were denatured and annealed to the primer for 10 min at 70°C and reverse transcribed for 3 h at 42°C. Before amplification, the reverse transcriptase was inactivated by heating to 70°C for 15 min, and RNA was hydrolyzed by incubation with 0.05 N NaOH at 70°C for 10 min, neutralized with 0.05 N HCl, and the cDNA precipitated with ethanol. The resulting cDNA products were dissolved in a final volume of 200 µl, and a 2-µl aliquot was used as template for subsequent quantification by real-time PCR amplification. PCR reactions were conducted in duplicate or triplicate in a total volume of 25 µl containing SYBR Green PCR Master Mix (Applied Biosystems, Grand Island, NY) and 0.1 µM of each primer. Gene specific primer sets for the various genes tested are shown in Supplemental Material, Table S1. Amplification was performed in an ABI 7500 (Applied Biosystems) where the reaction was heated to 95°C for 10 min, followed by 40 cycles of denaturation at 95°C for 15 seconds and annealing elongation at 60°C for 60 seconds. Detection of the fluorescent product was carried out during the 72°C extension period, and emission data were quantified using threshold cycle (C_t) values. C_t values for all genes analyzed were determined in biological

duplicates or triplicates, averaged, and means were determined from the average C_t values for each biological duplicate. All means were then normalized to values for Gapdh mRNA. PCR product specificity from each primer pair was confirmed using melting curve analysis and subsequent polyacrylamide gel electrophoresis.

RNA.seq data analysis.

All steps of library construction, cluster generation and HiSeq sequencing were performed with biological duplicate samples by the Genomics Sequencing Core of the Department of Environmental Health at the University of Cincinnati. Library construction was done with the TruSeq RNA sample preparation kit (Illumina, San Diego, CA) using 1 µg of total RNA with RNA integrity number ≥7.0 (Agilent 2100 Bioanalyzer) to purify poly-A containing mRNA with oligo-dT-attached magnetic beads. The purified mRNA was enzymatically fragmented and random hexamers-primed for first and second strand cDNA synthesis, followed by purification using Agencourt AMPure XP beads (Beckman Coulter, Florence, KY). Overhangs in the double-strand cDNA were blunt-ended by end repair, and adenylated with a single A-nucleotide at the 3' end to prevent self-ligation in the following ligation step. AMPure XP bead-purified fragments were ligated to sample-specific indexing adapters, and enriched by 10 cycles of PCR using adapter-specific primers. A 1-µl aliquot of purified PCR product—out of a total sequencing library of 30 µl—was analyzed in an Agilent Bioanalyzer using a DNA 1000 chip to check DNA size (~260 bp) and yield. To quantify the library concentration for clustering, the library was diluted 1:100 in a buffer containing 10 mM Tris-HCl, pH 8.0, 0.05% Tween 20, and analyzed by qPCR with a Kapa Library Quantification kit (KapaBiosystem, Woburn, MA) using ABI's 9700HT real-time PCR machine. Equal amounts of six individually indexed cDNA libraries were pooled for clustering in an Illumina cBot system flow cell at a concentration of 8

pM using Illumina's TruSeq SR Cluster Kit v3, and sequenced for 50 cycles using a TruSeq SBS kit on the Illumina HiSeq system. Each sample generated approximately 30 million sequence reads.

Sequence reads were de-multiplexed and exported to fastq files using Illumina's CASAVA 1.8 software. The reads were then aligned to the reference genome (mm10) using TopHat aligner (Trapnell et al. 2009). The counts of reads aligning to each gene's coding region were summarized using ShortRead (Morgan et al. 2009) and associated Bioconductor packages (GenomicFeatures, IRanges, GenomicRanges, Biostrings, Rsamtools) for manipulating and analysis of next-generation sequencing data and custom-written R (Ihaka and Gentleman 1996) programs. Differential gene expression analysis between AHR-positive and unselected cells was performed separately at each of the four different time points (Day 5, Day 8, Day 11 and Day 14). Statistical analysis to identify differentially expressed genes for each comparison was performed using the negative-binomial model of read counts as implemented in DESeq Biocondoctor package (Anders and Huber 2010). The same analysis was performed to compare TCDD- to control-treated AHR-positive cells at the same time points. Differential expression *p*-values were used in LRpath geneset enrichment analysis (Sartor et al. 2009a) to identify the top 100 Gene Ontology affected categories in each group. These Gene Ontologies were hierarchically clustered based on the LRpath enrichment z-score, with positive values denoting up-regulation and negative values, down-regulation. Clustering was done using the GENE-E algorithm (http://www.broadinstitute.org/cancer/software/GENE-E/). The gene expression data and results were deposited in GEO (Barrett et al. 2009) and can be accessed through Genomics Portals (http://GenomicsPortals.org) (Shinde et al. 2010) or at http://www.ncbi.nlm.nih.gov/geo/query/acc.cgi?acc=GSE47964.

Statistical Analysis.

Significant genes were selected by fdr- (false-discovery rate)-adjusted *p*-value<0.0001.

Results

The AHR is expressed in mesendoderm of early embryos and ES cell embryoid bodies.

AHR expression in the developing mouse embryo has been detected as early as GD 9.5 (Abbott et al. 1995). If the AHR has morphogenetic functions, its presence may be detectable at earlier times, in which case the choice of lineage and temporal-spatial expression pattern may give us an indication of the role that the AHR may play in embryonic development. Using immunofluorescence, we were able to document AHR expression at GD7.5, considerably earlier than previously described by others (Abbott et al. 1995). By this time, AHR is already clearly expressed in all three embryonic germ layers, ectoderm, mesoderm and endoderm, and in the surrounding decidual cells (Figure 1A). In all cell lineages of control embryos, the AHR localization was mainly cytosolic, but after treatment with 5µg/kg TCDD, it was both cytosolic and nuclear, becoming almost completely nuclear after treatment with 50 µg/kg TCDD (see Supplemental Material, Figure S1 for a higher magnification).

To study AHR expression at earlier developmental times, we used pluripotent ES cells differentiated *in vitro* on which temporal expression patterns of markers of all three germ layers can readily be followed (Beddington and Robertson 1989). To assess AHR expression, we used immunofluorescence of three-day-old embryoid bodies (EBs) treated with TCDD or control vehicle. Endodermal cells comprise the outer cell layers of the EB, as shown by the presence of the endodermal marker GATA4. The inner cell mass of the EB consists of mesodermal and

ectodermal cells, as shown by positive immunofluorescence with MF20 and keratin-18 antibodies, respectively. Control and TCDD-treated EBs show colocalization of AHR with GATA4 and MF20, and to a much lesser extent with keratin-18 (Figure 1B), suggesting that mesoderm and endoderm are the earliest cell lineages to express AHR.

At the mRNA level, *Ahr* expression is silent in ES cells and becomes detectable in two-day-old EBs, gradually increasing to a maximum after 6 days of differentiation, maintaining a constant level for the next 8-9 days (Figure 1C). Expression of Cyp1a1 mRNA follows a similar pattern, gradually increasing until differentiation day 6 when it reaches a maximum, slowly decreasing to a minimum by day 15 (Figure 1C). Interestingly, *Cyp1a1* expression is independent of treatment with an exogenous AHR ligand, suggesting that during these early developmental times, the AHR transcriptional functions are ligand-independent or regulated by an endogenous ligand. This finding is in good agreement with observations by others of constitutive *Cyp1a1* expression during early mouse embryonic development (Campbell et al. 2005). As expected, expression of the pluripotency markers *Oct4/Pou5f1* and *Nanog* declined gradually as the cells differentiate, down to their lowest level of expression on differentiation day 9 (Figure 1C).

AHR activation, knockdown, and inhibition all block cardiomyocyte lineage differentiation.

Pluripotent ES cells have the potential of generating most embryonic cell lineages (Doetschman et al. 1985), including cardiomyocytes (Yamashita et al. 2005). Differentiation of ES cells into cardiomyocytes can be traced microscopically by visual examination of differentiating EBs that spontaneously develop a contractile phenotype. Importantly, beating cardiomyocytes derived from ES cell embryoid bodies function in all manner as cardiac cells, forming stable intracardiac

grafts when injected into mice (Klug et al. 1996). Our previous work showed that treatment with 1 nM TCDD disrupted the beating phenotype (Wang et al. 2010). We extended this observation by further characterizing the consequences of treatment with AHR antagonists or molecular inhibitors on cardiomyocyte development. Continuous exposure of differentiating cells to TCDD led to a dose-dependent inhibition of beating, significantly different from control at 100 pM and 1 nM (Figure 1D, left panel). Knockdown of >80% AHR expression with a lentivirus expressing *Ahr*shRNA (see Supplemental Material, Figure S2), or treatment with the AHR antagonists TMF or CH223191 also significantly decreased the number of beating EB-derived cultures (Figure 1D, middle and right panels) without affecting cell survival. These results are a good indication that endogenous AHR signaling underlies homeostasis in cardiomyocyte differentiation and function, independently of the potential toxicity of its exogenous agonist. As this critical role can be disrupted by the opposing effects of AHR repression, inhibition or ligand-mediated activation, as shown, it is reasonable to conclude that the level of functional AHR during cardiomyogenesis is a critical determinant of differentiation. That is, that too little or too much of this protein adversely affects mesodermal lineage differentiation programs.

TCDD treatment disrupts the gene expression trajectories of cardiac markers.

We have previously observed that a 4-day treatment with TCDD after the completion of EB formation deregulates the expression of more than 50 homeobox genes, many by as much as 50- to 100-fold above or below control (Wang et al. 2010). To determine if any of these changes were responsible for the effect of TCDD on the beating phenotype, we dissected beating and non-beating regions of differentiating cultures treated with 1 nM TCDD or vehicle, and used qPCR to measure the gene expression levels of several markers relevant to cardiac function (Figure 2A; see also Supplemental Material, Table S2). Cells that continued to beat after TCDD

treatment showed no change in the expression of the markers tested relative to control vehicle treatment; however, TCDD treatment significantly repressed the expression of *Nkx2-5, Shox2, Myh6, Myh7, Cx40, Mlc2v, Hcn4* and *Nppa*, in non-beating cells and induced *Cyp1a1* expression in both beating and non-beating cells (Figure 2A). Interestingly, expression of *Pgp9.5*, a neuroendocrine marker and component of the cardiac conduction system (El Sharaby et al. 2001), was repressed under all conditions tested, indicating that cell of ectoderm lineage are not present in the beating or non-beating nodes selected. These data suggest that inhibition of the beating phenotype by TCDD treatment is independent of its role in xenobiotic metabolism and likely to be the consequence of silencing the expression of genes critical for the contractile phenotype.

Gene Ontology Annotations of Genes Differentially Expressed in AHR Positive Cardiomyocytes

Two major caveats must be considered when interpreting the data described above in the context of AHR-dependent gene expression. First, the differentiating cell population is a combination of cells of various lineages, where not more than 30 – 40% of all are cardiomyocytes (Wang et al. 2010); second, not all cells in the population express AHR. To insure that we track only cells positive for a functional AHR, we established a stable ES cell line, termed pAHRPuroIRESeGFP, that expresses the selection markers puromycin-resistance and eGFP under control of the *Cyp1a1* promoter, and therefore responds to TCDD treatment (see Supplemental Material, Figure S3A). These cells were greater than 90% pure (see Supplemental Material, Figure S3B) and did not over-expressed AHR relative to the parental ES cells (see Supplemental Material, Figure S3C, but expressed mesodermal markers characteristic of cardiomyocyte cells (see Supplemental Material, Figure S3D).

To characterize the effect of TCDD-dependent AHR activation on gene expression in AHR-positive pAHRPuroIRESeGFP cardiomyocytes, we used global gene expression profiling at different times of differentiation. Following 2 days of differentiation as hanging-drop EBs, we collected differentiated cells on days 5, 8, 11 and 14. To enrich for cells expressing AHR, cultures were selected for resistance to 3 µg/ml puromycin for 3 days prior to collection. A population of untransfected and unselected ES cells was grown and sampled in parallel. Gene expression changes across time were analyzed by comparing, (1) AHR-positive cells to unselected cells; and, (2) AHR-positive cells treated with 1 nM TCDD to the same cells treated with control vehicle. In each comparison, several thousand genes had significant expression differences with fdr-adjusted p-value<0.0001. These genes were used to identify the top 100 Gene Ontology (GO) affected categories in each group, which were hierarchically clustered by z-score using the GENE-E algorithm developed by the Broad Institute Cancer Group (http://www.broadinstitute.org/cancer/software/GENE-E/). Relative to unselected cells, AHR-positive cells showed a time-dependent decrease of expression of GO categories involved in cardiac differentiation and morphogenesis, increasingly lower expression of categories involved in WNT signaling, regulation of gastrulation, and gametogenesis, and high levels of expression of genes involved in drug and xenobiotic metabolism (Figure 2B; Supplemental Material, Table S3). TCDD treatment of AHR-positive cells identified three clusters of GO categories (Figure 2C). Cluster A includes categories involved in WNT and BMP signaling, cell adhesion and organ morphogenesis that are highly induced by TCDD-driven AHR activation at early time points but become repressed as differentiation proceeds. The opposite pattern is seen in cluster B, which includes genes involved in drug and xenobiotic metabolism. Cluster C includes genes with cardiac and neural differentiation functions, which are repressed by TCDD treatment

(Figure 2C; Supplemental Material, Table S4). Prominent pathways targeted by early AHR functions appear to be the regulation of gastrulation and WNT signaling during embryogenesis, which are disrupted by TCDD treatment at the earlier time points. Cardiac and neural differentiation, extracellular matrix formation and cell adhesion and migration are also early targets of TCDD in AHR positive cells. These data clearly illustrate the intricacy of the AHR role during differentiation and the multiplicity of pathways triggered by TCDD-driven AHR activation responses.

The AHR/TCDD Axis Disrupts the Expression of Homeobox Transcription Factors and Polycomb and Trithorax Group (PcG; TxG) Genes.

Our RNA.seq results indicated that a few thousand genes, comprising a significant fraction of the genome, were responsive to AHR/TCDD-mediated regulation. The most reasonable explanation for this finding is that the AHR is a master upstream regulator that controls the expression of homeobox transcription factors, shown to be responsible for the regulation of developmental gene expression in a tissue- and time-dependent fashion (Moreland et al. 2009). In agreement with this hypothesis, we found that 729 transcription factors, most homeodomain factors, were differentially expressed in TCDD-treated AHR-positive cells relative to control (Supplemental Material, Table S5). From this group, 100 factors with p-value<0.05 were specifically associated with cardiovascular development. To determine whether the AHR binding motif was present in the promoters of the genes coding for these factors, we used the TRANSFAC algorithm (Wingender 2008) to search for the presence of AHR Position Weight Matrix (PWM) motifs anywhere between -10,000 and +1,000 nucleotides from the Transcription Start Site (TSS). Approximately 50% of the genes with $\log_2$fold-change<-0.5 or >0.5 had at least one, but often more than one, AHR binding sites in this domain, whereas the other 50% did not. No

significant difference was observed between these two groups in either the level or the timing of differential expression (Figure 3A,B; Supplemental Material, Table S6).

PcG and TxG proteins constitute a group of critical regulators of epigenetic modifications affecting differentiation during development. They act coordinately or antagonistically to repress or promote transcription, respectively, throughout embryonic development (Schuettengruber et al. 2007). In agreement with the master regulatory role consistently shown by the AHR, our RNA.seq gene expression profiles detected the AHR/TCDD-dependent altered expression of 22 PcG and TxG genes in AHR positive cells (Supplemental Material, Figure S4; Supplemental Material, Table S7).

Functional analyses of gene expression changes resulting from activation of the AHR/TCDD axis.

To get a better understanding of the molecular and chemical interactions elicited by TCDD treatment and their phenotypic effects on AHR-positive cells, we input the 729 transcription factor RNA.seq data into the Ingenuity Knowledge Base (IPA; Ingenuity®Systems, http://www.ingenuity.com) to analyze the AHR/TCDD axis-driven effects on biological, canonical, and toxicological functions. The most significant change in biological functions took place in gene expression functions, as could be expected from the effects observed on homeobox transcription factors. Other biological changes affected several aspects of embryonic, cardiovascular system and tissue development, morphology, cell growth and cell proliferation. These changes were more significant at early stages of differentiation, as the –log(*p*-value) was in all cases greater at day 5 than at day 11 (Figure 4A). Several canonical functions were also significantly affected by TCDD treatment, including transcriptional regulation and various

signaling pathways, among them, WNT, TGFβ, AHR and cardiomyocyte differentiation via BMP receptors. As in the case of biological functions, these effects were more significant at early differentiation times (Figure 4B). The toxicological functions significantly affected by TCDD comprised a variety of cardiac endpoints that included congenital heart anomalies, cardiac dysfunction and proliferation, valvular stenosis, hypertrophy and heart failure, as well as cardiac, liver and renal hypoplasia (Figure 4C). These analyses only indicate that the pathways or functions are affected but do not inform as to the direction, activation or inhibition, of the effect. An Ingenuity Knowledge Base search for upstream regulatory molecules of the transcription factors involved in these functions found close to 200 such regulators, of which 18 - 20 had significant *p*-values. When these were ranked by z-score, two groups were evident (Table 1). One group comprised regulators that were predicted to be inhibited and included TGFβ, BMP2/4, WNT1/3A, FGFR2, NFκB, NKX2-5, Hedgehog and a few others that regulate differentiation pathways. The second group included regulators of pluripotency pathways, like SOX2, NANOG, KLF4, OCT4 and others, which, in contrast, were predicted to be activated. The overall effect of TCDD-driven AHR activation during the early stages of differentiation appears to be to maintain the pro-proliferative state of the ES cells and to inhibit their differentiation.

Discussion

Our results show that AHR activation by TCDD during differentiation of AHR-positive ES cells suppresses the development of the contractile cardiomyocyte phenotype. Concomitantly, activation of the AHR/TCDD axis disrupts the concerted expression of genes that regulate multiple differentiation pathways, including WNT and BMP, genes coding for developmental

processes such as gametogenesis, cardiac and neural differentiation, extracellular matrix formation and cell adhesion and migration, and genes encoding chromatin remodeling factors. Remarkably, a very similar pattern of TCDD regulatory effects have been recently described in the regeneration of adult zebrafish hearts (Hofsteen et al. 2013). As described in zebrafish (Lanham et al. 2012), this pattern of TCDD-induced regulatory effects seems to be more pronounced in the early stages of development, i.e. during days 5 and 8 of ES cell differentiation, and is accompanied by parallel changes in the expression of genes encoding homeobox transcription factors and PcG and TxG proteins. Furthermore, when beating and non-beating cardiomyocytes were analyzed separately after TCDD treatment, beating cardiomyocytes retained the expression of the cardiac markers *Nkx2-5, Shox2, Myh6, Myh7, Mlc2v* and *Cx40* regardless of treatment, whereas non-beating cells lost expression of these markers if they were treated with TCDD. These results are strong indication of a causal connection between AHR function, TCDD treatment and disruption of cardiomyocyte function. Moreover, since both AHR knockdown and its functional inhibition by antagonists suppress the beating phenotype just as efficiently as TCDD-dependent AHR activation, it is reasonable to conclude that too much or too little functional AHR is equally deleterious to cardiomyocyte function and that the amount of AHR protein itself is a determinant of cardiomyocyte homeostasis.

In addition to metabolic xenobiotic detoxification, the AHR plays an important role in maintenance of cellular homeostasis, often in the absence of a xenobiotic ligand (Bock and Kohle 2006). A physiological role for the receptor independent of xenobiotic ligand has been recognized in AHR null mice (Gonzalez and Fernandez-Salguero 1998), which show, among others, an impaired cardiovascular phenotype with retained fetal vascular structures in the liver and eye that fail to undergo apoptosis (Lahvis et al. 2005). Our results comparing gene

expression profiles of AHR-positive and unselected cells allow us to assess which developmental AHR functions may be independent of an exogenous ligand. Expression of genes controlling functions such as cardiac differentiation, regulation of WNT signaling, gametogenesis and gastrulation are enriched in AHR-positive cells relative to unselected cells. On the other hand, genes regulating extracellular matrix formation, cell adhesion and migration, neural differentiation and chromatin remodeling, are deregulated only after TCDD treatment of AHR-positive cells. These two groups of functions may respond to activation by endogenous and exogenous ligands, respectively, segregating physiological processes regulated by an endogenous ligand-activated AHR from toxicological or adaptive responses dependent on AHR activated by a xenobiotic ligand. In this context, it is significant that constitutive expression of *Cyp1a1*, a gene that is normally silent in the absence of ligand, is significantly derepressed during differentiation in the absence of TCDD, suggesting a response to either ligand-independent AHR activation or to activation by an endogenous ligand. Elevated constitutive *Cyp1a1* mRNA levels have also been found *in vivo* in fertilized mouse ova studies, and have been attributed to the need for catalytically active CYP1A1 that might ensure rapid metabolism of unwanted CYP1A1 substrates during critical moments of early development (Dey and Nebert 1998).

A major problem in the interpretation of data pertaining to individual regulatory networks in a mixed-lineage cell population like the differentiating ES cells is the lineage diversity. We adopted a promoter-mediated dominant selection system, previously established for the characterization of the cardiomyocyte transcriptome (Doss et al. 2007), to enrich for a population of AHR-positive cells which, when established as a continuously growing cell line, expressed mesodermal markers specific of the cardiomyocyte lineage. Global gene expression changes in

these cells showed the disruption of developmental WNT and BMP signaling pathways when treated with TCDD. BMP and WNT signaling during pre- and post-implantation embryonic development and their role during cardiomyocyte differentiation have long been recognized (Wang and Dey 2006). In mice, cooperative control of SMAD and WNT signaling pathways activates multiple transcription factors including *Gata4, Nkx2-5* and *Mef2c*, which control cardiac differentiation (Pal and Khanna 2006). Similarly, temporal modulation of canonical WNT signaling in human pluripotent stem cells results in robust cardiomyocyte differentiation (Lian et al. 2013). Importantly, extensive work in zebrafish has demonstrated the disruption of WNT signaling by TCDD (Hofsteen et al. 2013;Lanham et al. 2012;Mathew et al. 2009).

Homeodomain transcription factors specify the progression of tissue differentiation and embryonic identity during development (Wang et al. 2009). They encode transcription factors that control the expression of multiple developmental gene batteries. Disrupted expression or mutations in these genes result in severe to lethal outcomes for the organism (Wang and Dey 2006). In humans, mutations in 25 different homeobox transcription factors have been found in patients with congenital heart disease (McCulley and Black 2012); expression of 14 of these, *Cited2, Ets1, Foxh1, Gata4, Gata6, Hand1, Hand2, Hoxa1, Irx1, Nkx2-5, Nkx2-6, Pitx2* and *Tbx1*, is disrupted by TCDD in our mouse ES cell differentiation experiments. Two of these, *Nkx2-5* and *Gata4*, play a central role in cardiac development. *Nkx2-5* is genetically upstream of multiple genes essential for heart development; 33 heterozygous loss-of-function mutations in this gene have been reported to cause heart malformations in humans, including conduction delay and atrial septal dysmorphogenesis (Biben et al. 2000). In mice, homozygous *Nkx2-5* null embryos show arrested cardiac development after looping, poor development of blood vessels and disturbed expression of cardiac genes (Tanaka et al. 1999). Mutations in *Gata4* have been

associated with cardiac septal defects (Tomita-Mitchell et al. 2007). These transcription factors do not act alone; their cooperation and interdependent regulation is essential for cardiac development, such that disruption of the expression of any one gene leads to the imbalance of the overall transcriptional network. *Nkx2-5* and *Gata4* are mutual cofactors for each other; their co-expression leads to synergistic, rather than additive activation of target genes (Riazi et al. 2009) and promotion of cardiomyocyte differentiation (Hiroi et al. 2001). Hence, disruption of homeobox gene expression, a downstream target of the AHR/TCDD axis, is potentially a major component of the inhibition of cardiomyocyte function by TCDD. Interestingly, more than 50% of the homeobox genes regulated by the AHR do not have canonical AHR response sites in their promoters, suggesting that their regulation by the AHR may result from a complex combinatorial network of regulatory interactions that reaches beyond direct AHR signaling. Some of these interactions are likely to include epigenetic modifications of histone marks, as TCDD induces deregulation of PcG and TxG genes.

In conclusion, the present work provides strong support to the growing body of evidence in all experimental systems tested to date that the AHR is a major contributor to cardiovascular homeostasis. Changes in the homeostatic gene expression levels regulated by the AHR pathway disrupt cardiomyocyte differentiation, whether the AHR is in excess—if further activated by TCDD—or in defect—if inhibited by antagonists or shRNA. The significant role that the AHR plays in cardiovascular development makes the heart a most sensitive target of fetal environmental injury.

References

Abbott BD, Birnbaum LS, Perdew GH. 1995. Developmental expression of two members of a new class of transcription factors:I. Expression of aryl hydrocarbon receptor in the C57BL/6N mouse embryo. Dev Dynamics 204:133-143.

Anders S, Huber W. 2010. Differential expression analysis for sequence count data. Genome Biol 11:R106.

Aragon AC, Kopf PG, Campen MJ, Huwe JK, Walker MK. 2008. In utero and lactational 2,3,7,8-tetrachlorodibenzo-p-dioxin exposure:effects on fetal and adult cardiac gene expression and adult cardiac and renal morphology. Toxicol Sci 101:321-330.

Barker DJ. 2007. The origins of the developmental origins theory. J Intern Med 261:412-417.

Barrett T, Troup DB, Wilhite SE, Ledoux P, Rudnev D, Evangelista C, et al. 2009. NCBI GEO:archive for high-throughput functional genomic data. Nucleic Acids Res 37:D885-D890.

Beddington RS, Robertson EJ. 1989. An assessment of the developmental potential of embryonic stem cells in the midgestation mouse embryo. Development 105:733-737.

Biben C, Weber R, Kesteven S, Stanley E, McDonald L, Elliott DA, et al. 2000. Cardiac septal and valvular dysmorphogenesis in mice heterozygous for mutations in the homeobox gene Nkx2-5. Circ Res 87:888-895.

Bock KW, Kohle C. 2006. Ah receptor:dioxin-mediated toxic responses as hints to deregulated physiologic functions. Biochem Pharmacol 72:393-404.

Bruner-Tran KL, Osteen KG. 2011. Developmental exposure to TCDD reduces fertility and negatively affects pregnancy outcomes across multiple generations. Reprod Toxicol 31:344-350.

Campbell SJ, Henderson CJ, Anthony DC, Davidson D, Clark AJ, Wolf CR. 2005. The murine Cyp1a1 gene is expressed in a restricted spatial and temporal pattern during embryonic development. J Biol Chem 280:5828-5835.

Dey A, Nebert DW. 1998. Markedly increased constitutive CYP1A1 mRNA levels in the fertilized ovum of the mouse. Biochem Biophys Res Commun 251:657-661.

Doetschman TC, Eistetter H, Katz M, Schmidt W, Kemler R. 1985. The in vitro development of blastocyst-derived embryonic stem cell lines:formation of visceral yolk sac, blood islands and myocardium. J Embryol Exp Morphol 87:27-45.

Doss MX, Winkler J, Chen S, Hippler-Altenburg R, Sotiriadou I, Halbach M, et al. 2007. Global transcriptome analysis of murine embryonic stem cell-derived cardiomyocytes. Genome Biol 8:R56.

Dummer TJ, Dickinson HO, Parker L. 2003. Adverse pregnancy outcomes around incinerators and crematoriums in Cumbria, north west England, 1956-93. J Epidemiol Community Health 57:456-461.

El Sharaby AA, Egerbacher M, Hammoda AK, Bock P. 2001. Immunohistochemical demonstration of Leu-7 (HNK-1), Neurone-specific Enolase (NSE) and Protein-Gene Peptide (PGP) 9.5 in the developing camel (Camelus dromedarius) heart. Anat Histol Embryol 30:321-325.

Gertsenstein M, Nutter LM, Reid T, Pereira M, Stanford WL, Rossant J, et al. 2010. Efficient generation of germ line transmitting chimeras from C57BL/6N ES cells by aggregation with outbred host embryos. PLoS One 5:e11260.

Gonzalez FJ, Fernandez-Salguero P. 1998. The aryl hydrocarbon receptor:studies using the AHR-null mice. Drug Metab Dispos 26:1194-1198.

Gu YZ, Hogenesch JB, Bradfield CA. 2000. The PAS superfamily:sensors of environmental and developmental signals. Annu Rev Pharmacol Toxicol 40:519-561.

Hiroi Y, Kudoh S, Monzen K, Ikeda Y, Yazaki Y, Nagai R, et al. 2001. Tbx5 associates with Nkx2-5 and synergistically promotes cardiomyocyte differentiation. Nat Genet 28:276-280.

Hofsteen P, Mehta V, Kim MS, Peterson RE, Heideman W. 2013. TCDD inhibits heart regeneration in adult zebrafish. Toxicol Sci 132:211-221.

Ihaka P, Gentleman R. 1996. R:A language for data analysis and graphics. J. Comp.ut. Graph. Stat.5: 299-314.

Ivnitski-Steele ID, Walker MK. 2005. Inhibition of neovascularization be environmental agents. Cardiovasc. Toxicol. 5:215-226.

Klug MG, Soonpaa MH, Koh GY, Field LJ. 1996. Genetically selected cardiomyocytes from differentiating embronic stem cells form stable intracardiac grafts. J Clin Invest 98:216-224.

Kopf PG, Walker MK. 2009. Overview of developmental heart defects by dioxins, PCBs, and pesticides. J Environ Sci Health C Environ Carcinog Ecotoxicol Rev 27:276-285.

Kuehl KS, Loffredo CA. 2006. A cluster of hypoplastic left heart malformation in Baltimore, Maryland. Pediatr Cardiol 27:25-31.

Lahvis GP, Pyzalski RW, Glover E, Pitot HC, McElwee MK, Bradfield CA. 2005. The aryl hydrocarbon receptor is required for developmental closure of the ductus venosus in the neonatal mouse. Mol Pharmacol 67:714-720.

Lai TJ, Liu X, Guo YL, Guo NW, Yu ML, Hsu CC, et al. 2002. A cohort study of behavioral problems and intelligence in children with high prenatal polychlorinated biphenyl exposure. Arch Gen Psychiatry 59:1061-1066.

Lanham KA, Peterson RE, Heideman W. 2012. Sensitivity to dioxin decreases as zebrafish mature. Toxicol Sci 127:360-370.

Lian X, Zhang J, Azarin SM, Zhu K, Hazeltine LB, Bao X, et al. 2013. Directed cardiomyocyte differentiation from human pluripotent stem cells by modulating Wnt/beta-catenin signaling under fully defined conditions. Nat Protoc 8:162-175.

Lund AK, Goens MB, Kanagy NL, Walker MK. 2003. Cardiac hypertrophy in aryl hydrocarbon receptor null mice is correlated with elevated angiotensin II, endothelin-1, and mean arterial blood pressure. Toxicol Appl Pharmacol 193:177-187.

Mathew LK, Sengupta S, Franzosa JA, Perry J, La DJ, Andreasen EA, et al. 2009. Comparative expression profiling reveals an essential role for raldh2 in epimorphic regeneration. J Biol Chem 284:33642-33653.

McCulley DJ, Black BL. 2012. Transcription factor pathways and congenital heart disease. Curr Top Dev Biol 100:253-277.

Moreland RT, Ryan JF, Pan C, Baxevanis AD. 2009. The Homeodomain Resource:a comprehensive collection of sequence, structure, interaction, genomic and functional information on the homeodomain protein family. Database 2009:bap004:1-8.

Morgan M, Anders S, Lawrence M, Aboyoun P, Pages H, Gentleman R. 2009. ShortRead:a bioconductor package for input, quality assessment and exploration of high-throughput sequence data. Bioinformatics 25:2607-2608.

Pal R, Khanna A. 2006. Role of smad- and wnt-dependent pathways in embryonic cardiac development. Stem Cells Dev 15:29-39.

Plavicki J, Hofsteen P, Peterson RE, Heideman W. 2013. Dioxin inhibits zebrafish epicardium and proepicardium development. Toxicol Sci 131:558-567.

Reyes H, Reiz-Porszasz S, Hankinson O. 1992. Identification of the Ah receptor nuclear translocator protein (Arnt) as a component of the DNA binding form of the Ah receptor. Science 256:1193-1195.

Riazi AM, Takeuchi JK, Hornberger LK, Zaidi SH, Amini F, Coles J, et al. 2009. NKX2-5 regulates the expression of beta-catenin and GATA4 in ventricular myocytes. PLoS One 4:e5698.

Sartor MA, Leikauf GD, Medvedovic M. 2009a. LRpath:a logistic regression approach for identifying enriched biological groups in gene expression data. Bioinformatics 25:211-217.

Sartor MA, Schnekenburger M, Marlowe JL, Reichard JF, Wang Y, Fan Y, et al. 2009b. Genomewide analysis of aryl hydrocarbon receptor binding targets reveals an extensive array of gene clusters that control morphogenetic and developmental programs. Environ Health Perspect 117:1139-1146.

Schecter A, Cramer P, Boggess K, Stanley J, Papke O, Olson J, et al. 2001. Intake of dioxins and related compounds from food in the U.S. population. J Toxicol Environ Health A 63:1-18.

Schnekenburger M, Peng L, Puga A. 2007. HDAC1 bound to the Cyp1a1 promoter blocks histone acetylation associated with Ah receptor-mediated trans-activation. Biochim Biophys Acta 1769:569-578.

Schuettengruber B, Chourrout D, Vervoort M, Leblanc B, Cavalli G. 2007. Genome regulation by polycomb and trithorax proteins. Cell 128:735-745.

Shinde K, Phatak M, Johannes FM, Chen J, Li Q, Vineet JK, et al. 2010. Genomics Portals:integrative web-platform for mining genomics data. BMC Genomics 11:27.

Tanaka M, Chen Z, Bartunkova S, Yamasaki N, Izumo S. 1999. The cardiac homeobox gene Csx/Nkx2.5 lies genetically upstream of multiple genes essential for heart development. Development 126:1269-1280.

Tomita-Mitchell A, Maslen CL, Morris CD, Garg V, Goldmuntz E. 2007. GATA4 sequence variants in patients with congenital heart disease. J Med Genet 44:779-783.

Trapnell C, Pachter L, Salzberg SL. 2009. TopHat:discovering splice junctions with RNA-Seq. Bioinformatics 25:1105-1111.

Walker MK, Catron TF. 2000. Characterization of cardiotoxicity induced by 2,3,7, 8-tetrachlorodibenzo-p-dioxin and related chemicals during early chick embryo development. Toxicol Appl Pharmacol 167:210-221.

Wang H, Dey SK. 2006. Roadmap to embryo implantation:clues from mouse models. Nat Rev Genet 7:185-199.

Wang KC, Helms JA, Chang HY. 2009. Regeneration, repair and remembering identity:the three Rs of Hox gene expression. Trends Cell Biol 19:268-275.

Wang Y, Fan Y, Puga A. 2010. Dioxin Exposure Disrupts the Differentiation of Mouse Embryonic Stem Cells into Cardiomyocytes. Toxicol Sci 115:225-237.

Wingender E. 2008. The TRANSFAC project as an example of framework technology that supports the analysis of genomic regulation. Brief Bioinform 9:326-332.

Wu Q, Ohsako S, Baba T, Miyamoto K, Tohyama C. 2002. Effects of 2,3,7,8-tetrachlorodibenzo-p-dioxin (TCDD) on preimplantation mouse embryos. Toxicology 174:119-129.

Yamashita JK, Takano M, Hiraoka-Kanie M, Shimazu C, Peishi Y, Yanagi K, et al. 2005. Prospective identification of cardiac progenitors by a novel single cell-based cardiomyocyte induction. FASEB J 19:1534-1536.

Table 1. Predicted activation state of upstream transcriptional regulators in TCDD-treated AHR-positive differentiating ES cells.

Differentiation Day	Activation State	Regulator	z-score	p-value
Day 5	Inhibited	APLNR	-2.1	5.05E-07
	Inhibited	BMP2	-2.4	1.57E-06
	Inhibited	BMP4	-2.6	5.93E-17
	Inhibited	FGFR2	-2.8	9.26E-11
	Inhibited	GLI2	-2.4	3.31E-07
	Inhibited	Hedgehog	-2.7	1.42E-19
	Inhibited	MLL	-2.2	1.04E-12
	Inhibited	NFkB	-2.2	5.33E-07
	Inhibited	NKX2-5	-1.1	1.37E-08
	Inhibited	SHH	-3.1	5.48E-13
	Inhibited	TGFB1	-2.1	2.03E-07
	Inhibited	TNF	-2.8	1.75E-07
	Inhibited	WNT1	-2.9	1.92E-10
	Inhibited	WNT3A	-2.9	7.34E-11
Day 5	Activated	GNL3	2.4	2.31E-08
	Activated	POU5F1	2.3	1.85E-19
	Activated	RNF2	2.2	3.01E-11
	Activated	SOX2	2.3	1.78E-20
Day 8	Inhibited	APLNR	-2.4	1.86E-09
	Inhibited	BMP4	-3.3	2.81E-23
	Inhibited	BMPR1A	-2.7	2.87E-09
	Inhibited	CTNNB1	-2.2	2.91E-22
	Inhibited	EPHB4	-2.5	8.04E-09
	Inhibited	FGFR2	-2.9	4.73E-08
	Inhibited	GLI2	-2.4	7.45E-12
	Inhibited	MLL	-3.5	2.00E-29
	Inhibited	NKX2-5	-0.5	2.98E-08
	Inhibited	STAT3	-3.1	3.77E-08
	Inhibited	TGFB1	-4.2	6.39E-15
	Inhibited	tretinoin	-2.5	3.41E-42
	Inhibited	WNT11	-2.2	2.71E-08
Day 8	Activated	GNL3	2.6	3.28E-14
	Activated	PHC2	2.6	3.85E-13
	Activated	POU4F1	2.5	1.16E-17
	Activated	POU4F2	2.4	5.39E-19
	Activated	POU5F1	2.7	5.31E-26
	Activated	RNF2	3.1	1.27E-16
	Activated	SOX2	2.3	3.87E-26
Day 11	Inhibited	ARID4B	-2.1	8.03E-07
	Inhibited	BMP2	-2.5	3.10E-15
	Inhibited	BMP7	-2.2	2.25E-08
	Inhibited	BMPR1A	-2.6	5.76E-07
	Inhibited	GLI3	-2.4	1.48E-11
	Inhibited	HOXA9	-2.2	9.81E-10
	Inhibited	MLL	-3.1	2.58E-30
	Inhibited	NKX2-5	-0.7	5.94E-08

Differentiation Day	Activation State	Regulator	z-score	p-value
Day 11 (cont.)	Inhibited	SMO	-2.1	7.57E-10
	Inhibited	STAT3	-2.6	4.71E-07
	Inhibited	TGFB1	-3.4	1.48E-10
	Inhibited	tretinoin	-2.8	1.63E-36
Day 11	Activated	KLF4	2.1	3.18E-07
	Activated	NANOG	2.1	2.68E-18
	Activated	OCT4	2.1	1.14E-09
	Activated	PHC2	2.4	8.70E-11
	Activated	POU4F2	2.2	7.99E-15
	Activated	POU5F1	2.5	1.19E-25
	Activated	RNF2	2.1	1.99E-15
	Activated	SOX2	2.3	1.07E-22
Day 14	Inhibited	ARID4A	-2.1	1.31E-06
	Inhibited	ARID4B	-2.1	5.62E-07
	Inhibited	BMP2	-2.5	4.31E-10
	Inhibited	EPHB4	-2.1	6.34E-11
	Inhibited	GLI1	-2.4	8.28E-07
	Inhibited	GSC	-2.1	2.56E-06
	Inhibited	HDAC	-2.2	3.26E-10
	Inhibited	HOXA9	-2.2	1.61E-08
	Inhibited	miR-34a-5p	-2.2	2.72E-08
	Inhibited	MLL	-2.9	8.01E-27
	Inhibited	NKX2-5	-0.7	2.98E-08
	Inhibited	SPRY1	-2.2	3.88E-07
	Inhibited	STAT3	-3.1	4.67E-07
	Inhibited	TGFB1	-3.3	5.52E-08
	Inhibited	tretinoin	-3.1	1.49E-32
Day 14	Activated	PHC2	2.4	5.07E-11
	Activated	SOX2	2.2	4.68E-22

Figure Legends

Figure 1. Detection of AHR in embryos, EBs and cardiomyocytes. (A) Embryos were exposed to corn oil vehicle and 5 or 50 μg/kg TCDD on GD5.5 and examined by immunofluorescence on GD7.5. E: endoderm; Ec: ectoderm; M: mesoderm. **(B)** Immunofluorescence detection of lineage markers in 3-day-old EBs treated with TCDD or left untreated. Antibodies used were directed against GATA4, cardiomyocytes (MF20), keratin-18 and AHR. From left to right, Columns 1 and 2 show immunofluorescence with AHR or the individual marker antibodies respectively; Column 3, the merge of columns 1 and 2; and Column 4 the merge of Column 3 with the DAPI nuclear stain. Magnification in both micrographs was 20X; bar = 20 μm. **(C)** Expression pattern of *Ahr*, *Cyp1a1*, *Oct4/Pou5f1* and *Nanog* in differentiating EBs. Log_2 qPCR mRNA levels were normalized to *Gapdh* and expressed as the ratio to the corresponding levels in ES cells (differentiation day 0). Data are means of three independent experiments ± SD. **(D)** Effect of TCDD treatment (Left), AHR knockdown (Middle) and AHR antagonists TMF and CH223191, used at 10 μM each (Right) on cardiomyocyte contractility. Three-day-old EBs were allowed to differentiate and examined daily under the microscope for the presence of a rhythmic beating phenotype. (*) $p<0.05$; (**) $p<0.01$; (***) $p<0.001$ differences to DMSO control by Bonferroni-corrected ANOVA..

Figure 2. Cardiac marker expression in beating and non-beating differentiated ES cells and clustering analyses of gene expression changes regulated by AHR. (A) Beating and non-beating areas from 12-day-old EBs treated with 1 nM TCDD or untreated were separated under a dissecting microscope. Relative mRNA expression levels were normalized as in Figure1 and shown as means ± SD. BC, beating control; BT, beating, TCDD treated; NBC, non-beating

control; NBT, non-beating, TCDD treated; (#):NBC or NBT significantly different ($p<0.05$) from BC or BT, respectively; (*) BT or NBT significantly different ($p<0.05$) from BC or NBC, respectively by one-way ANOVA. Hierarchical clustering of top 100 Gene Ontology categories by z-score using the GENE-E algorithm (see text and Methods) **(B)** Heatmap of AHR-positive differentiated cells compared to unselected differentiated cells. **(C)** Heatmap of AHR-positive differentiated cells treated with 1 nM TCDD compared to the same cells treated with control vehicle. Salient categorical groups in each cluster are indicated.

Figure 3. RNA.seq expression changes of the 100 homeobox transcription factors associated with cardiovascular development deregulated by the AHR/TCDD axis. Genes positive (A) or negative (B) for AHR PWM anywhere between coordinates -10,000 and +1,000 NT from the TSS.

Figure 4. Functional analyses of gene expression changes induced by TCDD in AHR-positive cardiomyocytes. The Ingenuity Knowledge Base (IPA; Ingenuity®Systems, http://www.ingenuity.com) was used to analyze the TCDD effects on (A) biological; (B) canonical; and (C) toxicological functions on day-5 and -11 of differentiation.

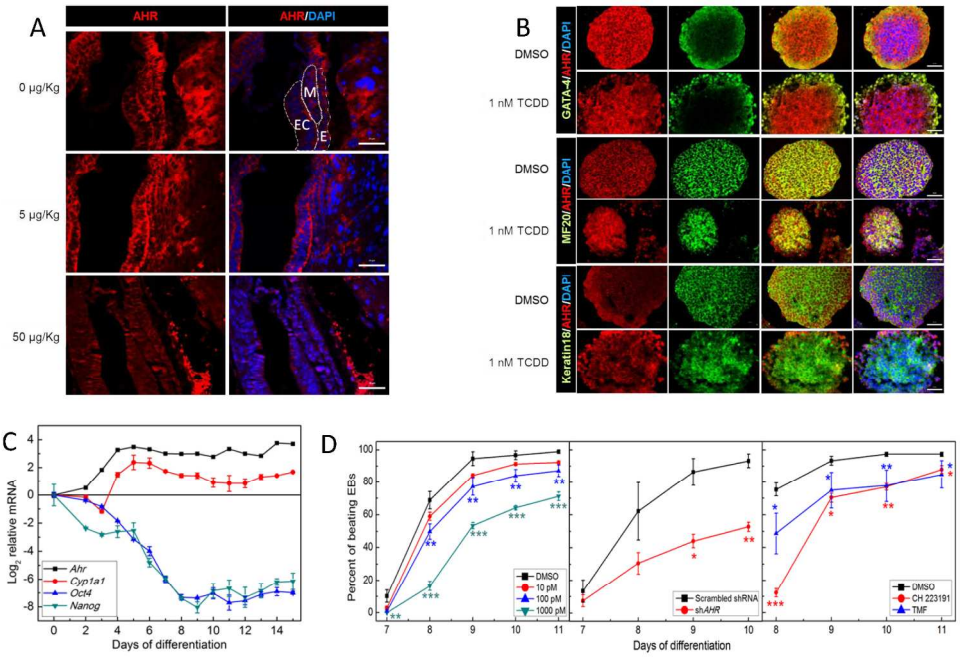

Figure 1

221x158mm (300 x 300 DPI)

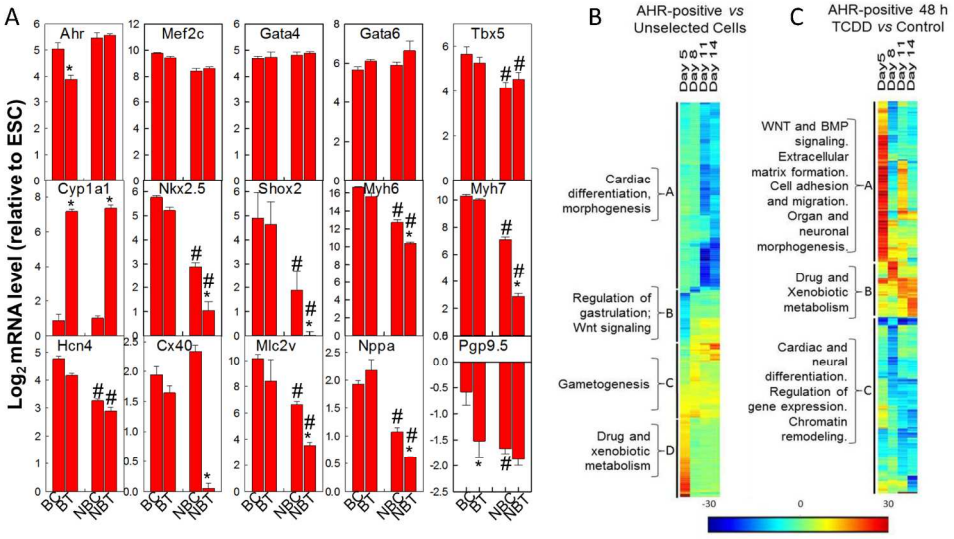

Figure 2
238x131mm (300 x 300 DPI)

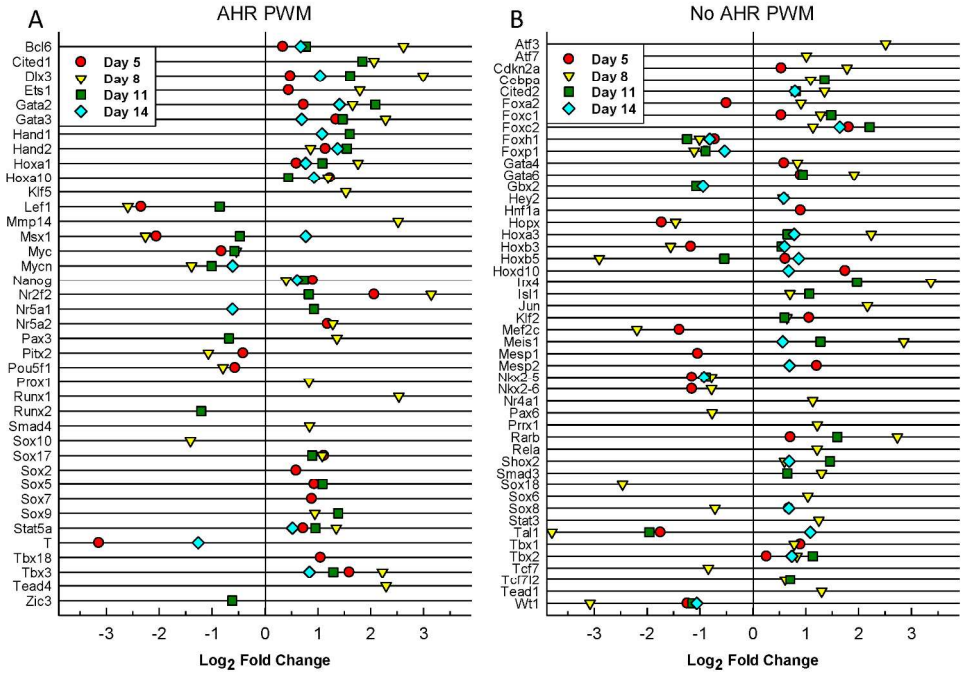

Figure 3
234x163mm (300 x 300 DPI)

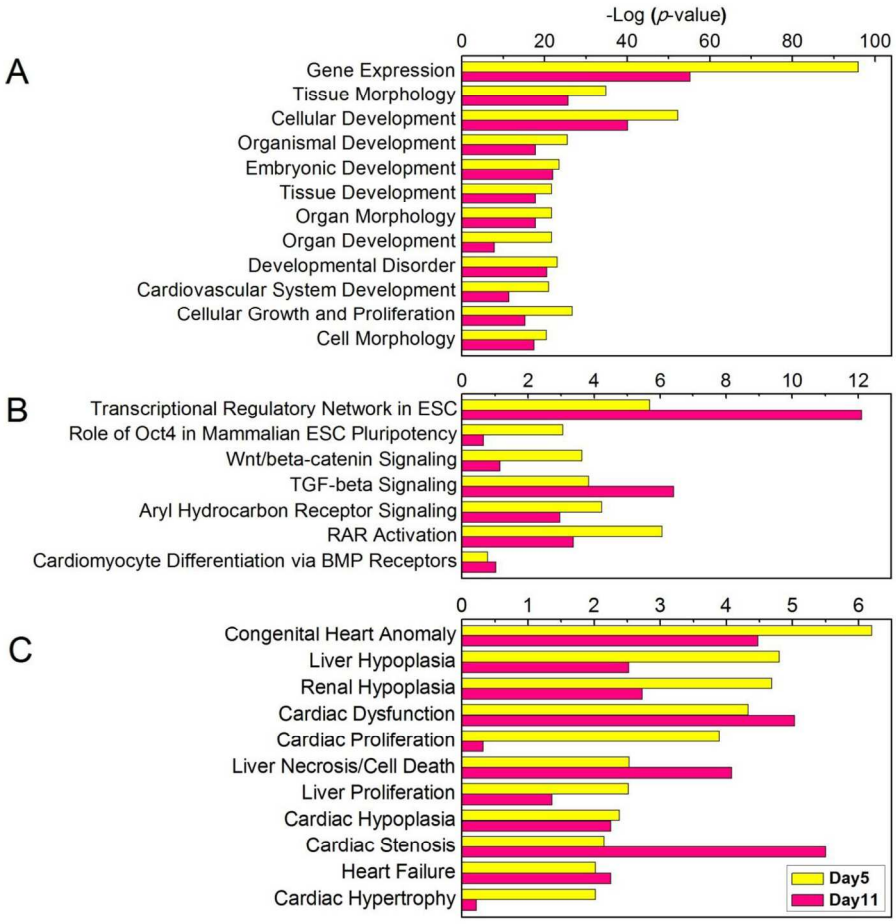

Figure 4
172x166mm (300 x 300 DPI)